Scientific Research Publishing

Open Journal of Fluid Dynamics, 2023, 13, 61-79
https://www.scirp.org/journal/ojfd
ISSN Online: 2165-3860
ISSN Print: 2165-3852

Linear and Nonlinear Stokes Waves Theory: Numerical Hydrodynamic and Energy Studies

Alpha Malick Ndiaye, Fadel Diop, Samba Dia, Cheikh Mbow

Laboratoire de Mécanique des Fluides et Transferts, Département de Physique, Faculté des Sciences et Techniques, Université Cheikh Anta Diop (UCAD), Dakar, Sénégal
Email: alphamalick@hotmail.fr

How to cite this paper: Ndiaye, A.M., Diop, F., Dia, S. and Mbow, C. (2023) Linear and Nonlinear Stokes Waves Theory: Numerical Hydrodynamic and Energy Studies. *Open Journal of Fluid Dynamics*, **13**, 61-79.
https://doi.org/10.4236/ojfd.2023.131005

Received: February 25, 2023
Accepted: March 27, 2023
Published: March 30, 2023

Abstract

The increase of wave energy in electricity production is an objective shared by many countries to meet growing demand and global warming. To analyze devices capable of converting the energy of sea waves into electrical energy, it is important to master the various theories of gravity waves and generation. We will in our work consider a numerical waves tank for an amplitude $A = 0.5$, a wavelength $\lambda = 0.25$, an average height $H_e = 10$ and a Froude number fixed at 1×10^5. Numerical wave channel analysis is used to reproduce the natural phenomenon of wave propagation in an experimental model. Wave makers are usually used to generate waves in the channel. In theory, the influence of an incident wave can be considered, as in the case of our study. In this study, the evolution of the hydrodynamic parameters and the energy transported in one wavelength can be determined by calculation. A change of variable will be done in this work to facilitate the writing of the boundary conditions at the free surface and at the bottom. The nonlinear Stokes theory will be studied in this case in order to provide hydrodynamic solutions through the Navier-Stokes equations to finally deduce the energetic results. To do this, the finite difference method will be used for the hydrodynamic results such as the velocity potential and the free surface elevation and the trapezium method of Newton for the energetic results. Thus, we will determine the energetic potential according to the decrease in the slope of the tank. To do this, we will take as values of beta representing the inverse of the slope of the tank, $\beta = 100$, $\beta = 105$, $\beta = 110$ and $\beta = 115$.

Keywords

Waves Tank, Energy, Waves, Gravity Waves, Navier-Stokes, Numerical, Nonlinear Stokes Theory

1. Introduction

The increase of renewable energy in electricity production is an objective shared by many countries to meet growing demand and global warming. In this energy mix, the part of marine energies remains very low. Most of the technologies are not yet mature and only off-shore wind power today participates in the production of energy of marine origin. However, the swell can be an exploitable source of energy for the production of electricity. For this purpose; over the past thirty years, a number of wave energy systems (wave energy recovery systems) have been proposed and studied, all over the world but mainly in Europe. According to Cruz and Sarmento (2004), the oceans, containing the greatest of all natural resources, have enormous energy potential, which can contribute significantly to the growing energy needs at the global level. One way to investigate this potential is to perform computer simulations and laboratory experiments. For this, we use models that physically describe the phenomenon. To analyze devices capable of converting the energy of sea waves into electrical energy, it is important to master the various theories of gravity waves and their generation. The nonlinear Stokes theory is the oldest and the most studied, because it's possible to understand most of the phenomena related to nonlinear waves. An analytical solution not being accessible for such a theory, we will have recourse to numerical methods or disturbances to bring solutions concerning this theory. In the case of the nonlinear water wave problem, Stokes (1847) was the first to develop a finite amplitude wave theory [1] using the perturbation method to account for nonlinear terms [2]. Since then, many theories describing wave motions using this method have been derived to higher-order approximations for finite values of wave amplitude. This has led to an important specialized bibliography that has accumulated over the years. Since that time, the works carried out on the subject have not ceased to be published until today. Christensen *et al.* (2002) [3] offer a review of the various numerical methods currently used to study breaking waves. Thus, we distinguish the methods from the kinetic theory, the models based on the Boussinesq equations, the models based on the theory of potential flows and those based on the Navier-Stokes equations. In order to predict high-order wave loads for a cylindrical, single-tower platform exposed to regular waves, Klepsvik (1995) [4] solved the first-order problem using the computer program Wave Analysis MIT (WAMIT) to get the extra mass and wave dampening. Then, he used the principle of superposition to find the pitch response due to second-order and higher-order wave loads. Also, Molin *et al.* (2005) [5] and Rahman *et al.* (1999) [6] focused on the study of the interaction of second-order waves with, respectively, the vertical square cylinder and the circular cylinder. Similarly, a time domain method is used to analyze the interactions of water waves and a group or network of cylinders. Nonlinear free surface boundary conditions are satisfied based on the perturbation method up to the second order. The first and second-order velocity potential problems at each time step are solved by a Finite Element Method (FEM). In order to analyze the inhomogeneous term involved

in the free surface condition for the diffraction of second-order waves on a pair of cylinders, Bhatta (2005) [7] derived the second-order scattered potential. Under the assumption of a large spacing between the two cylinders, the waves scattered by a cylinder can be replaced in the vicinity of the other cylinder by equivalent plane waves accompanied by non-planning correction terms. Yang *et al.* (2013) [8] formulated a complete second-order theory for coupling numerical and physical waves in wave tanks [9]. The new formulation is presented in a unified form that includes both progressive and evanescent modes and covers piston and flap-type wave generator configurations. Second-order vane travel correction enables enhanced nonlinear wave generation in the physical wave reservoir based on target digital solutions. The performance and efficiency of the new model are first evaluated theoretically based on second-order Stokes waves. Mangoub (1992) [10] presented a numerical study on the behavior of a vortex concentration in the swell. The concentrated vortex can be due both to the presence of natural and artificial obstacles, such as the bases of structures, for example. They treated separately the calculation of the swell and the free surface on the one hand and that of the evolution of the vortex on the other hand. They did not consider the generation of the tourbillon: the bottom is chosen flat. Their goal was to develop a numerical computer code that allows following the evolution of a vortex concentration in the nonlinear wave field. Loukill *et al.* (2016) [11] presented a perturbation method coupled with the finite difference method for solving the problem of wave propagation in a wave tank. In this work, they proposed a semi-analytical or rather semi-numerical method for the resolution of nonlinear wave propagation. The principle of the method is to apply the perturbation method to the nonlinear problem at the start, which allowed them to have verified linear problems for the different orders (Navfey, 1973; Hinsh, 1991). These nonlinear problems also present a great difficulty which concerns the writing of the boundary conditions on the free surface in an evolving domain. The problems being unsteady, these transformations will therefore be evolutionary. The numerical resolution of transformed linear problems is carried out by the method of finite differences. We present solutions for higher orders (order 1, order 2...). A comparison with Stokes' exact solution is presented (Subsbelles *et al.*, 1981) [12]. Bebassakis and Athanassoulis [13] extended the second-order Stokes theory to the case of a generally shaped bottom profile connecting two half-strips of constant (but possibly different) depths based on hydrodynamic parameters. Wave energy and power are commonly used and referenced in the literature for wave transformation as the wave approaches the shore, as well as for analysis of general flow dynamics. For more information, see Horikawa (1988), Dean and Dalrymple (1992), Van Rijn (1994), Kamphuis (2000) and CEM (2002), among others. The main objective of marine energy is its transformation into electricity to meet the high energy demand and global warming (Babarit & Mouslim [14]; Michard, Cosquer & Dufour [15]). To do this, it is necessary to know the evolution of hydrodynamic parameters which are the essence of energy transport in

the case of waves. Cheung and Childress [16] and Erikson [17] have calculated the hydrodynamic coefficients with the Finite Element Method (FEM) or the Finite Volume Method (FVM).

Our goal is to study the temporal evolution of hydrodynamic parameters such as: the free elevation surface and the potential field for different variations of the bottom slope numerically under the nonlinear approximation. Finally, we will deduce from these results the evolution of the energy as a function of time and the variation of the slope of the bottom. To do this, we will simulate our model from a numerical wave tank initially actuated by an incident linear Stokes wave. The determination of the energy requires beforehand a detailed and explicit study of the hydrodynamic aspect, namely the evolution of the free surface elevation and the distribution of the velocity potential in the wave tank.

To do this, we will first describe the physical model to be studied and describe the calculation through the mathematical formulation. The equations obtained being nonlinear, we will finally approach the numerical formulation to give the results.

2. Mathematical Formulation

2.1. System Description and Problem Formulation in the Physical Domain

In order to clarify the approach used, we will expose our problem by proposing a numerical wave tank to describe the calculation. During the last decade, research has been done to develop numerical wave tanks [18]. Research has developed different numerical methods to simulate ocean waves. Wei *et al.* [19] and Chawla [20] implemented a source function method to generate ocean waves, based on the Boussinesq model. Based on the 2D form of the Navier-Stokes equations, Dong and Huang [21] established a 2D numerical wave reservoir to simulate small amplitude waves and solitary waves. Lu [22] numerically simulated the overtopping of waves against levees in the case of regular waves. We consider a 2D and irrotational flow of a non-viscous and incompressible fluid under the influence of a Stokes wave in a wave tank of length L, wavelength λ and amplitude A (see **Figure 1**). The bottom condition follows a linear evolution given by

$$z = h(x) = \frac{h_0}{L} x \tag{1}$$

We propose to numerically solve the weakly nonlinear system of Equation (2) representing the propagation of a Stokes wave and which are written in terms of the velocity potential ϕ and free surface elevation $\eta(x;t)$ and consisting respectively of

- **Laplace equation**
- **Kinematic free surface condition**: Water particles cannot cross the free surface. To satisfy the condition of particle velocity $z = \eta$ must be equal to the normal speed at the free surface.
- **Dynamic free surface condition**: The pressure at the free surface is zero for

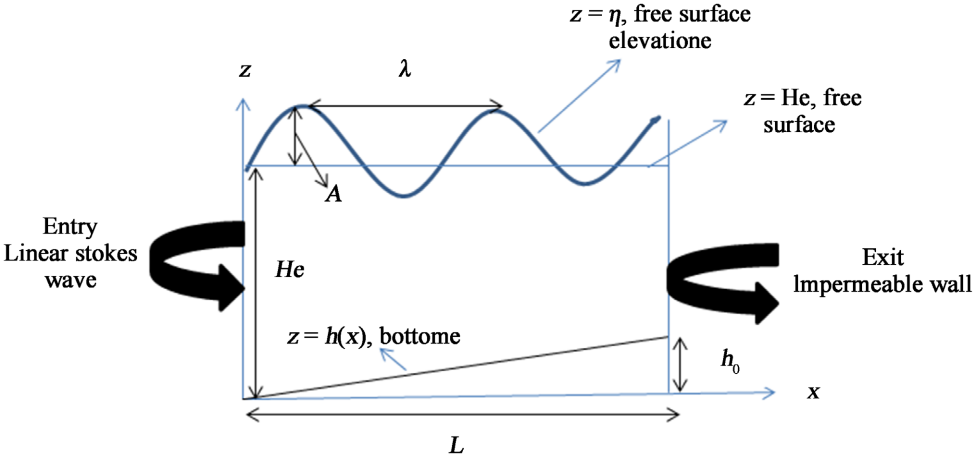

Figure 1. Geometry of the problem.

any position and time. Basically consists of applying the Bernoulli equation to the free surface.

- **Bottom condition**: The bottom can be considered as variable and impermeable.

$$\begin{cases} \dfrac{\partial^2\phi}{\partial x^2}+\dfrac{\partial^2\phi}{\partial z^2}=0 & h(x)<z<\eta(x;t);0\le x\le L \\ \dfrac{\partial\eta}{\partial t}=-\dfrac{\partial\phi}{\partial x}\dfrac{\partial\eta}{\partial x}+\dfrac{\partial\phi}{\partial z} & z=\eta(x;t);0\le x\le L \\ \dfrac{\partial\phi}{\partial t}+\dfrac{1}{2}\left[\left(\dfrac{\partial\phi}{\partial x}\right)^2+\left(\dfrac{\partial\phi}{\partial z}\right)^2\right]+g\eta=0 & z=\eta(x;t);0\le x\le L \\ \dfrac{\partial\phi}{\partial z}-\dfrac{\partial\phi}{\partial x}\dfrac{\partial h}{\partial x}=0 & z=h(x);0\le x\le L \end{cases} \tag{2}$$

To remove the difficulties of knowing the treatment of the problem in unsteady regime and the determination of the conditions at the entry and exit boundaries, we will consider an incident linear wave upstream of the tank propagating on a flat bottom of constant depth He of which we know all its hydrodynamics characteristics and which will drive the movement. The hydrodynamic parameters of the incident wave are given by

$$\eta(x;t)=A\cos(kx-\omega t) \tag{3}$$

$$\phi(x;z;t)=\frac{A\omega}{k}\frac{\cosh\left[k(H_e+z)\right]}{\sinh(kH_e)}\sin(kx-\omega t) \tag{4}$$

Thus, we can give the initial conditions and complete with the boundary conditions by giving the entry and exit conditions for the free surface elevation η and the velocity potential ϕ.

- **Initial condition**

At $t=0$, the tank is initially disturbed by a linear Stokes wave

$$\eta(x;t=0)=H_e+A\cos(kx) \tag{5}$$

$$\phi(x;z;t=0)=\frac{Ag}{\omega}\frac{\cosh\left[k(z+H_e)\right]}{\sinh(kH_e)}\sin(kx) \tag{6}$$

- **Entry condition**

For the entry conditions, we consider that the incident wave upstream of the tank is a linear Stokes wave and that its impact at the entrance creates the wave motion at $t > 0$. We then have for the entry conditions the free surface elevation and the velocity potential

$$\eta(0;t) = A\cos(\omega t) + H_e \tag{7}$$

$$\phi(0;z;t) = \frac{Ag}{\omega}\frac{\cosh\left[k\left(z+H_e\right)\right]}{\sinh\left(kH_e\right)}\sin\left(-\omega t\right) \tag{8}$$

- **Exit condition**

For the exit conditions, we consider a solid impermeable wall. We will then have for the exit conditions of the free surface elevation and of the velocity potential

$$\eta(L;t) = A\cos(kL - \omega t) + H_e \tag{9}$$

$$\frac{\partial\phi}{\partial x} = \frac{\partial\phi}{\partial z} = 0 \tag{10}$$

2.2. Energy

Wave propagation in water gives it a kinetic energy, due to the mouvements of the particles, as well as a variation of its potential energy due to the displacement of the free surface. The hydrodynamic results obtained will allow us to deduce the energy contained in a wavelength λ inside the tank per width unit which is the sum of the potential and kinetic energies which are given respectively by

$$E_p = \int_0^{\lambda}\int_{h(x)}^{\eta}\rho g z\mathrm{d}x\mathrm{d}z \tag{11}$$

By taking as a reference level for the potential energy at the bottom.

And

$$E_c = \frac{1}{2}\int_0^{\lambda}\int_{h(x)}^{\eta}\rho\left[\left(\frac{\partial\phi}{\partial x}\right)^2 + \left(\frac{\partial\phi}{\partial z}\right)^2\right]\mathrm{d}x\mathrm{d}z \tag{12}$$

3. Dimensionless Study

Considering the multiplicity of the parameters which intervene in the whole of the system of equation of our mathematical model, it would be useful to find a technique to reduce them. To do this, we can agglomerate them in the form of dimensionless grouping having a physical significance and which allow

- Obtain information on the solution before solving the problem.
- To optimize a possible experimental approach.

Dimensionless quantities and number

To each quantity of the equations which govern the flow, one can correspond to a dimensionless quantity from the characteristic quantities. Indeed, we have:

$$t = t^* t_0;\quad x = x^* L;\quad z = z^* h_0;\quad \eta = \eta^* h_0;\quad \phi = \phi^*\frac{L^2}{t_0};\quad k = k^*/L$$

$$A = A^* h_0;\quad H_e = H_e^* h_0$$

With t_0, L and h_0 respectively the time, the characteristic length along the x axis and the characteristic length along the z axis.

We thus obtain from the dimensionless system dimensionless numbers, namely the Froude number and a number characteristic of the geometry of the channel which we will note β.

- The Froude number being the ratio between the forces of inertia and the forces of gravity and its expression is given by

$$\frac{1}{Fr} = \frac{gh_0 t_0^2}{L^2} = \frac{gh_0}{L^2\omega^2} \tag{13}$$

- The characteristic number of the geometry of the problem is given by

$$\beta = \frac{L}{h_0} \tag{14}$$

This number tells us about the shape of the slope of the wave tank.

This problem as it is proposed, essentially presents the following difficulties: nonlinear, unsteady problem, written on a domain with curved and evolutionary border.

3.1. Dimensionless Formulation in Curvilinear Coordinates $(\chi^*;\zeta^*)$

In order to facilitate the processing of boundary conditions on these boundaries, an orthogonal curvilinear coordinate system will be used. In this work we use a system of curvilinear coordinates which makes it possible to marry the shape of the free surface at all times and to take account of the irregularity of the bottom. This transformation facilitates the writing of boundary conditions on the irregular and evolving boundaries of the domain. The homotopic transformation T which transforms the physical region (D) into a rectangular domain (Dt) at each dimensionless instant t^* is defined by

$$\begin{cases} T: D \to Dt \\ \left(x^*, z^*\right) \mapsto \left(\chi^*, \xi^*\right) \end{cases}$$

$$\text{With } \chi^* = x^*; \zeta^* = \frac{z^* - h^*\left(x^*\right)}{\eta^*\left(x^*; t^*\right) - h^*\left(x^*\right)}; t^* = t^* \tag{15}$$

We then move from the physical domain to a rectangular mathematical domain to describe the numerical calculation as shown in **Figure 2**.

The new system to be solved consisting of the Laplace equation; the conditions at the boundaries of the tank and the initial conditions will be written according to the curvilinear coordinates in the transformed and dimensionless domain.

3.2. Dimensionless Equations in Curvilinear Coordinates System

- **Laplace equation for** $0 < \zeta^* < 1; 0 \le \chi^* \le 1$

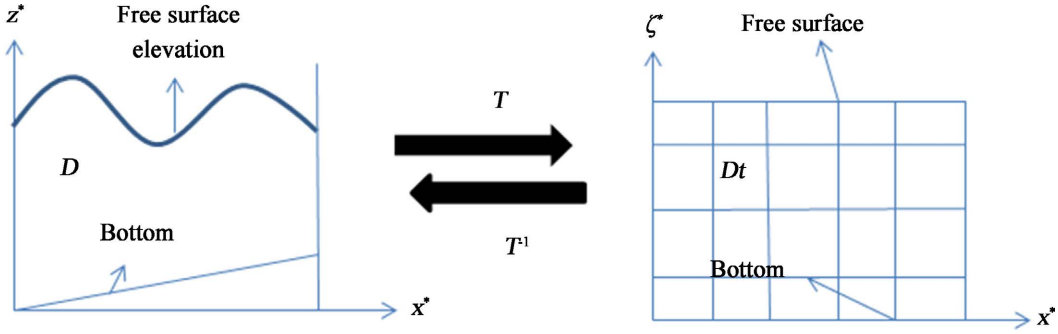

Figure 2. Transformation of the physical domain into rectangular domain.

$$\frac{\partial^2\phi^*}{\partial\chi^{*2}}+\frac{\partial^2\phi^*}{\partial\zeta^{*2}}\left\{\left(\frac{\beta}{\eta^*\left(\chi^*;t^*\right)-h^*\left(\chi^*\right)}\right)^2+G^{*2}\left(\chi^*;\zeta^*\right)\right\}+2G^*\left(\chi^*;\zeta^*\right)\frac{\partial^2\phi^*}{\partial\chi^*\partial\zeta^*}$$
$$+\frac{\partial\phi^*}{\partial\zeta^*}\left\{\left(\frac{1}{\eta^*\left(\chi^*;t^*\right)-h^*\left(\chi^*\right)}\right)^2\left[2\left(1-\frac{\partial\eta^*\left(\chi^*;t\right)}{\partial\chi^*}\right)\left(\zeta^*\left(1-\frac{\partial\eta^*\left(\chi^*;t\right)}{\partial\chi^*}\right)-1\right)\right.\right. \quad (16)$$
$$\left.\left.-\zeta^*\left(\eta^*\left(\chi^*;t^*\right)-h^*\left(\chi^*\right)\right)\frac{\partial^2\eta^*\left(\chi^*;t^*\right)}{\partial\chi^{*2}}\right]\right\}=0$$

With

$$G^*\left(\chi^*;\zeta^*\right)=\frac{1}{\eta^*\left(\chi^*;t^*\right)-h^*\left(\chi^*\right)}\left(\zeta^*\left(1-\frac{\partial\eta^*\left(\chi^*;t\right)}{\partial\chi^*}\right)-1\right) \quad (17)$$

- **Free surface kinematic condition for** $\zeta^*=1;0\le\chi^*\le1$

$$\frac{\partial\eta^*\left(\chi^*;t^*\right)}{\partial t^*}-\frac{\partial\phi^*}{\partial\zeta^*}\frac{1}{\eta^*\left(\chi^*;t^*\right)-h^*\left(\chi^*\right)}\left[\left(\frac{\partial\eta^*\left(\chi^*;t^*\right)}{\partial\chi^*}\right)^2+\beta^2\right] \quad (18)$$
$$+\frac{\partial\phi^*}{\partial\chi^*}\frac{\partial\eta^*\left(\chi^*;t^*\right)}{\partial\chi^*}=0$$

- **Free surface Dynamic condition for** $\zeta^*=1;0\le\chi^*\le1$

$$\frac{\partial\phi^*}{\partial t^*}+\frac{1}{2}\left[\left(\frac{\partial\phi^*}{\partial\chi^*}-\frac{1}{\eta^*\left(\chi^*;t^*\right)-h^*\left(\chi^*\right)}\frac{\partial\eta^*\left(\chi^*;t\right)}{\partial\chi^*}\frac{\partial\phi^*}{\partial\zeta^*}\right)^2\right. \quad (19)$$
$$\left.+\beta^2\left(\frac{1}{\eta^*\left(\chi^*;t^*\right)-h^*\left(\chi^*\right)}\frac{\partial\phi^*}{\partial\zeta}\right)^2\right]+\frac{1}{Fr}\eta^*\left(\chi^*;t^*\right)=0$$

- **Bottom condition for** $\zeta^*=0;0\le\chi^*\le1$

$$\frac{\partial\phi^*}{\partial\zeta^*}\frac{1}{\eta^*\left(\chi^{*};t^*\right)-h^*\left(\chi^*\right)}\left[\frac{1+\beta^2}{\beta^2}\right]-\frac{1}{\beta^2}\frac{\partial\phi^*}{\partial\chi^*}=0 \quad (20)$$

- **Initial condition for** $0<\chi^*<1;0<\zeta^*<1$

At $t^*=0$,

$$\eta^*\left(\chi^*;t^*=0\right)=H_e^*+A^*\cos\left(k^*\chi^*\right) \tag{21}$$

$$\phi^*\left(\chi^*;\zeta^*;t^*=0\right) = \frac{1}{Fr}A^*\frac{\cosh\left[\frac{k^*}{\beta}*\left(\zeta^*\left(\eta^*\left(\chi^*;t^*=0\right)-\chi^*\right)+\chi^*+H_e^*\right)\right]}{\sinh\left(k^*H_e^*/\beta\right)}\sin\left(k^*\chi^*\right) \tag{22}$$

- **Entry condition for** $x^*=0;0<\zeta^*<1$

$$\eta^*\left(0;t^*\right)=A^*\cos\left(t^*\right)+H_e^* \tag{23}$$

$$\phi^*\left(0;\zeta^*;t^*\right)=\frac{1}{Fr}A^*\frac{\cosh\left[\left(k^**\zeta^*\eta^*\left(0;t^*\right)+k^*H_e^*\right)/\beta\right]}{\sinh\left(k^*H_e^*/\beta\right)}\sin\left(-t^*\right) \tag{24}$$

- **Exit condition for** $x^*=1;0<\zeta^*<1$

$$\eta^*\left(1;t^*\right)=A^*\cos\left(k^*-t^*\right)+H_e^* \tag{25}$$

$$\frac{\partial\phi^*}{\partial\chi^*}+\frac{1}{\eta^*-1}\left(\zeta^*\left(1-\frac{\partial\eta^*}{\partial\chi^*}\right)-1\right)\frac{\partial\phi^*}{\partial\zeta^*}=0 \tag{26}$$

The kinematic condition and the Laplace equation give respectively the free surface elevation and the velocity potential.

3.3. Dimensionless Energy in Curvilinear Coordinates System

The dimensionless potential and kinetic energies in the new system calculated on a wavelength λ are respectively given by

$$E_p^*=\frac{1}{Fr\beta}\int_0^{\lambda^*}\int_0^1\left(\zeta^*\left(\eta^*-\chi^*\right)+\chi^*\right)\left|J^*\right|\mathrm{d}\chi^*\mathrm{d}\zeta^* \tag{27}$$

$$E_c^*=\frac{1}{2\beta}\int_0^{\lambda^*}\int_0^1\left[\left(\frac{\partial\phi^*}{\partial\chi^*}+G^*\left(\chi^*,\zeta^*\right)\frac{\partial\phi^*}{\partial\zeta^*}\right)^2+\left(\frac{1}{\eta^*\left(\chi^*;t^*\right)-h^*\left(\chi^*\right)}\beta\frac{\partial\phi^*}{\partial\zeta^*}\right)^2\right]\left|J^*\right|\mathrm{d}\chi^*\mathrm{d}\zeta^* \tag{28}$$

With $\left|J^*\right|$ represents the dimensionless Jacobian of the transformation and is given by

$$\left|J^*\right|=\eta^*-\chi^* \tag{29}$$

Notice that the reference of potential energy is taken at the bottom.

4. Numerical Procedure

The discretization of the differential equations makes it possible to transform these differential equations into algebraic equations where the continuous variations of the variables of the flow are represented by values at discrete points. Discrete locations in space are represented by nodal points (or nodes) chosen from a numerical grid (mesh) that subdivides the flow domain as shown in **Fig-**

ure 3. The discretization procedure makes approximations to the spatial derivatives of the variables of the flow present in the differential equation, at each node of the grid.

The spatial partial derivatives obtained from the equations of the system will be approximated by classical finite difference schemes [23] all of order 2, namely the scheme decentered downstream or upstream for the parietal conditions and the scheme centered inside of the domain (Laplace condition). The choice of the upstream or downstream off-center diagram will be justified according to the geometry of our problem and will be elucidated in the discretization calculation. The purpose of this choice is to ensure that the movement of the fluid involved is confined within the calculation domain.

To approximate the time derivative, we want to use an implicit two-level scheme of the Euler type with a constant time step δt.

Numerical Resolution Technic

To determine the numerical results of the free surface elevation and the potential field inside the domain we will solve the matrix systems respectively from the kinematic condition at the free surface and from the Laplace condition using iterative methods which are based on the repeated application of a simple algorithm leading to eventual convergence after a finite number of repetitions (iterations). We will use in this work the iterative method of relaxation line by line of Gauss-Siedel [24] by using the Successive Over Relaxation (SOR) [25]. The principle of iterative methods consists in seeking the solution of the system using a series of successive approximations. By giving an arbitrary vector of components $\left(\bar{\mathcal{F}}_i\right)^k$, we can find $\left(\bar{\mathcal{F}}_i\right)^{k+1}$ at the next iteration. The process is stopped when the following convergence criterion is met Equation (30)

$$\frac{\sum_{i=1}^{i=i_m}\left|\left(\bar{\mathcal{F}}_i\right)^{k+1}-\left(\bar{\mathcal{F}}_i\right)^k\right|}{\sum_{i=1}^{i=i_m}\left|\left(\bar{\mathcal{F}}_i\right)^{k+1}\right|}\leq \varepsilon_{\bar{\mathcal{F}}} \tag{30}$$

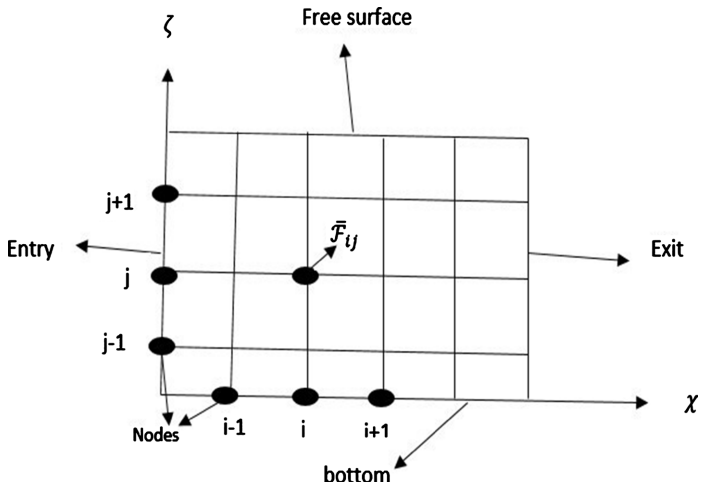

Figure 3. Meshing of the study area.

Besides the criterion of convergence of the iterative processes Equation (30) it is also necessary to define a criterion for stopping the calculation program. We stop the calculations.

When, at high times, the variations of our functions between two consecutive times are very small. Under these conditions, we take as stopping criterion

$$\min\left\{e_\eta; e_\phi\right\} \le Cr_{\bar{\mathcal{F}}} \tag{31}$$

$$\text{Avec} \quad e_{\bar{\mathcal{F}}} = \frac{\sum_{i=1}^{i=i_m}\left|\left(\bar{\mathcal{F}}_i\right)^{n+1} - \left(\bar{\mathcal{F}}_i\right)^{n}\right|}{\sum_{i=1}^{i=i_m}\left|\left(\bar{\mathcal{F}}_i\right)^{n+1}\right|} \tag{32}$$

For the numerical calculation of the energy, we will approach all the integrals using Newton's trapezium method [26].

5. Results and Discussion

In this chapter, we present the numerical results obtained from the calculation code that we developed with the FORTRAN 2003 Double Precision software and that simulates the propagation of a non-linear Stokes wave in a variable bottom wave tank.

5.1. Numerical Results and Interpretations

These results mainly concern the evolution of the free surface and the distribution of the velocity potential over time. Thus, we will deduce the numerical evolution of the energy as a function of the slope over time. The fixed dimensionless physical parameters of the problem in our modelling are listed in Table 1 for a Froude number fixed at 1×10^5.

The results presented are from simulations performed for $\beta = 100$, $\beta = 105$, $\beta = 110$ and $\beta = 115$. The error criteria for the convergence of the iterative calculations for the free surface elevation and the velocity potential are given in Table 2.

After writing the calculation program in FORTRAN language, we will visualize the numerical results using MATLAB software to see the influence of the

Table 1. Dimensionless physicals parameters.

Dimensionless physicals parameters		
Amplitude	**Mean height**	**Wavelength**
$A = 0.5$	$H_e = 10$	$\lambda = 0.25$

Table 2. Error criteria for the convergence of iterative calculations

	Hydrodynamics parameters	
	Free surface elevation	**Velocity potential**
$\varepsilon_{\bar{\mathcal{F}}}$	0.001	0.001

variation of the slope on the temporal evolution of the hydrodynamic parameters and the energy.

5.2. Free Surface Elevation and Velocity Potential Profile for β = 100

Figure 4 shows the longitudinal variations of the free surface and velocity potential at different times. At the initial time, the tank is influenced by a periodic Stokes wave with a crest height equal to the depth of the trough. In the course of time the crest height decreases in favour of an increase in the depth of the trough. Thus, the exit condition being an impermeable wall has the effect of causing the wave to dip while decreasing the height of the crests and increasing the depth of the troughs over time.

The propagation of the wave in the tank influences the movement of the particles from the free surface to the bottom by considering the velocity potential (Figure 4 (left)). Thus, for $t^* \le 2.5\times10^{-3}$ (Figure 4(a)), there is a periodic movement of the particles with a maximum intensity at the free surface which decreases until it is cancelled out as it approaches the bottom. The movement is under the crests in the direction of propagation of the wave (positive potential) and in the opposite direction under the troughs (negative potential). In the course of time, the decrease in the height of the crest in favour of the increase in the depth of the trough decreases the intensity of the movement under the crest and increases that under the trough. At the final time (Figure 4(d)), there is a movement only under the trough and the movement under the crest is cancelled. This is because the exit condition totally reflects the wave and the movement of the particles. The crest height and the trough depth influence the movement of the particles. Decreasing the crest height decreases the movement below the crest. Increasing the trough depth increases the movement below the trough.

5.3. Influence of β on Hydrodynamics Parameters

Figures 5-7 show the influence of β on the hydrodynamic parameters η and ϕ at different times.

Figure 5 and Figure 6 show that for times less than 1.7 and for $\beta \ge 105$ the variations of β do not affect the longitudinal variations of the free surface. However, it can be observed that there is a small decrease in the intensity of movement at the free surface under the crests and troughs as β increases.

Figure 7 shows that for $t^* = 1.7$, an increase in β for $\beta \ge 105$ results in a slight decrease in the height of the crest and a trough depth that increases more and more as we approach the exit and there is a small decrease in the intensity of movement at the free surface. The movement is only in the opposite direction of the wave propagation under the troughs (negative potential).

Note also that the values of $\beta \le 105$ do not affect the profile of the free surface for $t^* \prec 1.7$ or slightly for $t^* = 1.7$ There is also a decrease in the intensity of

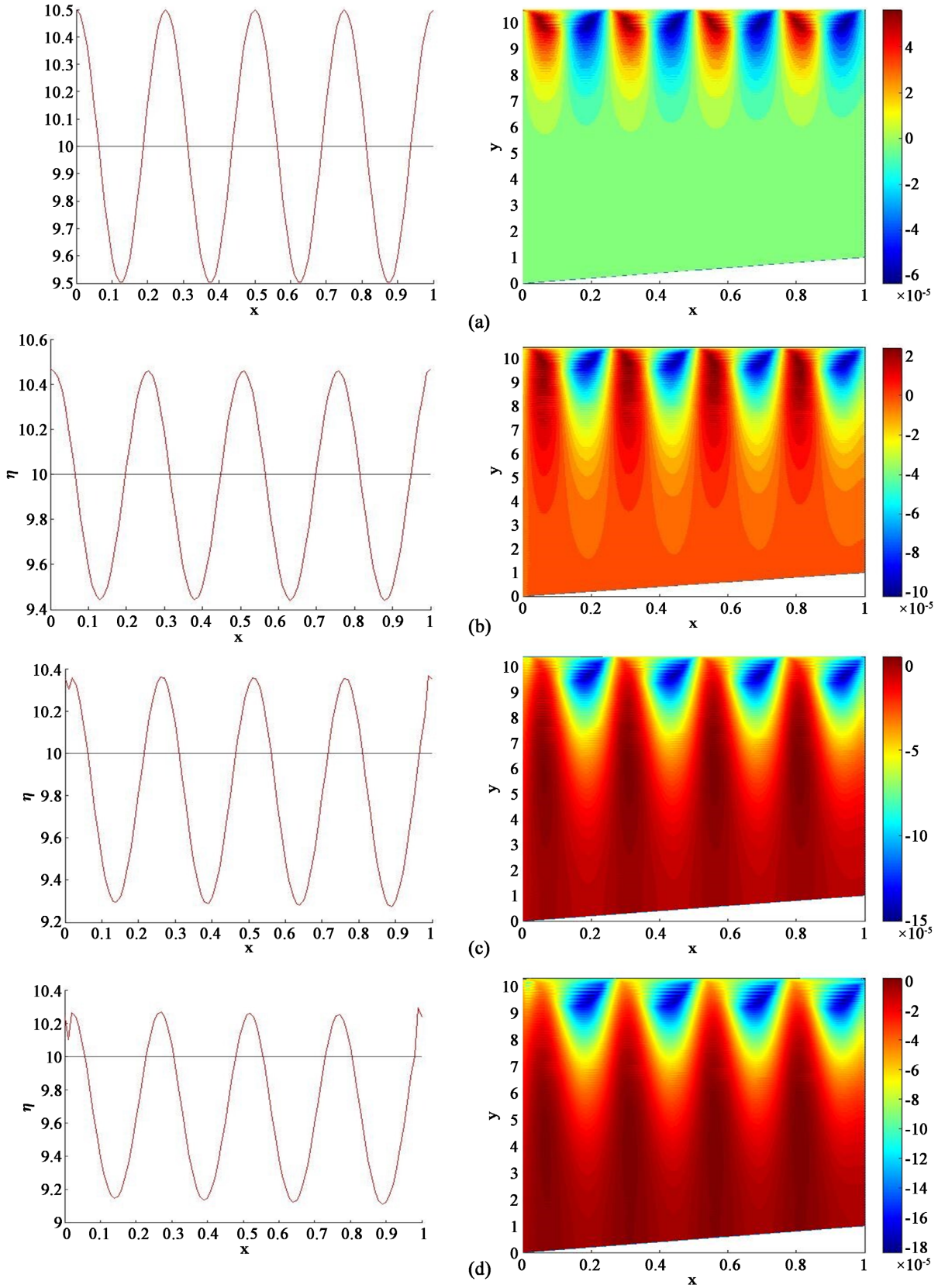

Figure 4. Free surface (left) and velocity potential (right) at different times. (a) $t^* = 2.5\times10^{-3}$; (b) $t^* = 0.36$; (c) $t^* = 0.8$; (d) $t^* = 1.7$.

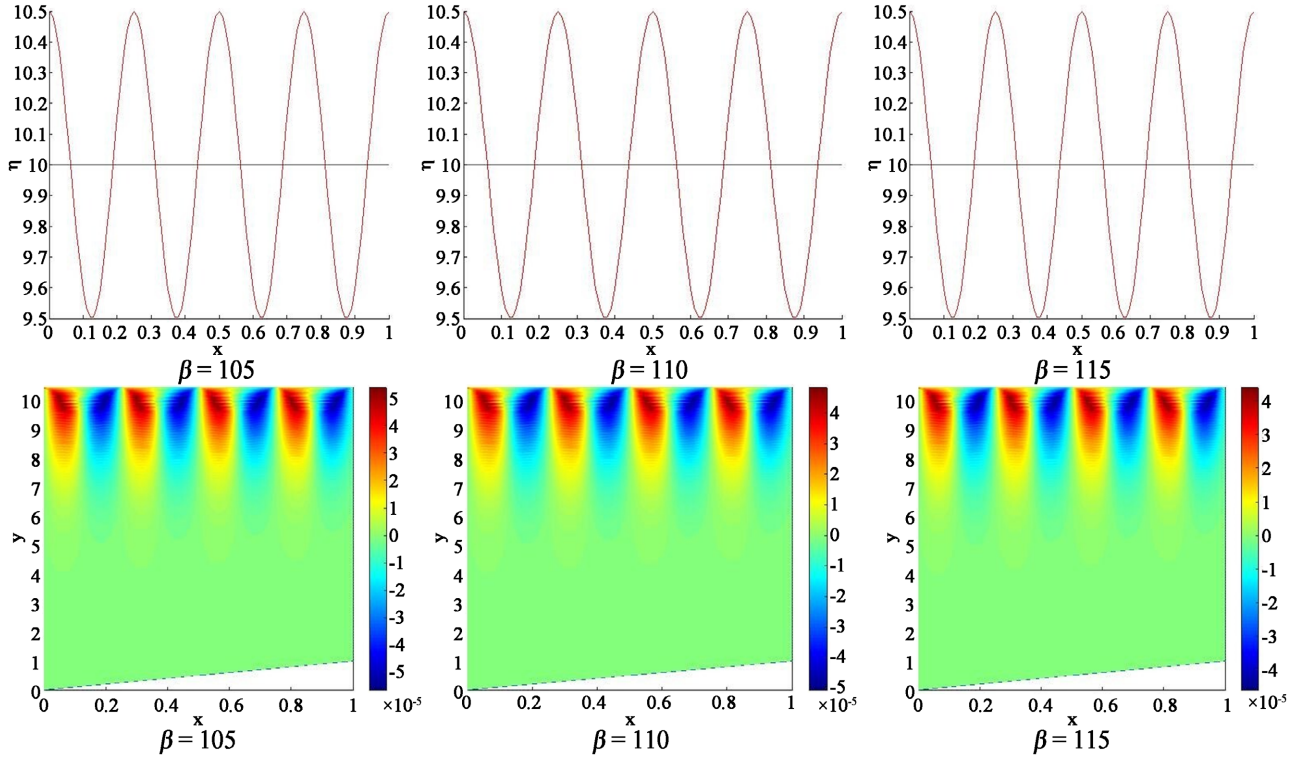

Figure 5. Free surface and velocity potential profiles for $t^* = 2.5\times10^{-3}$ for different values of β.

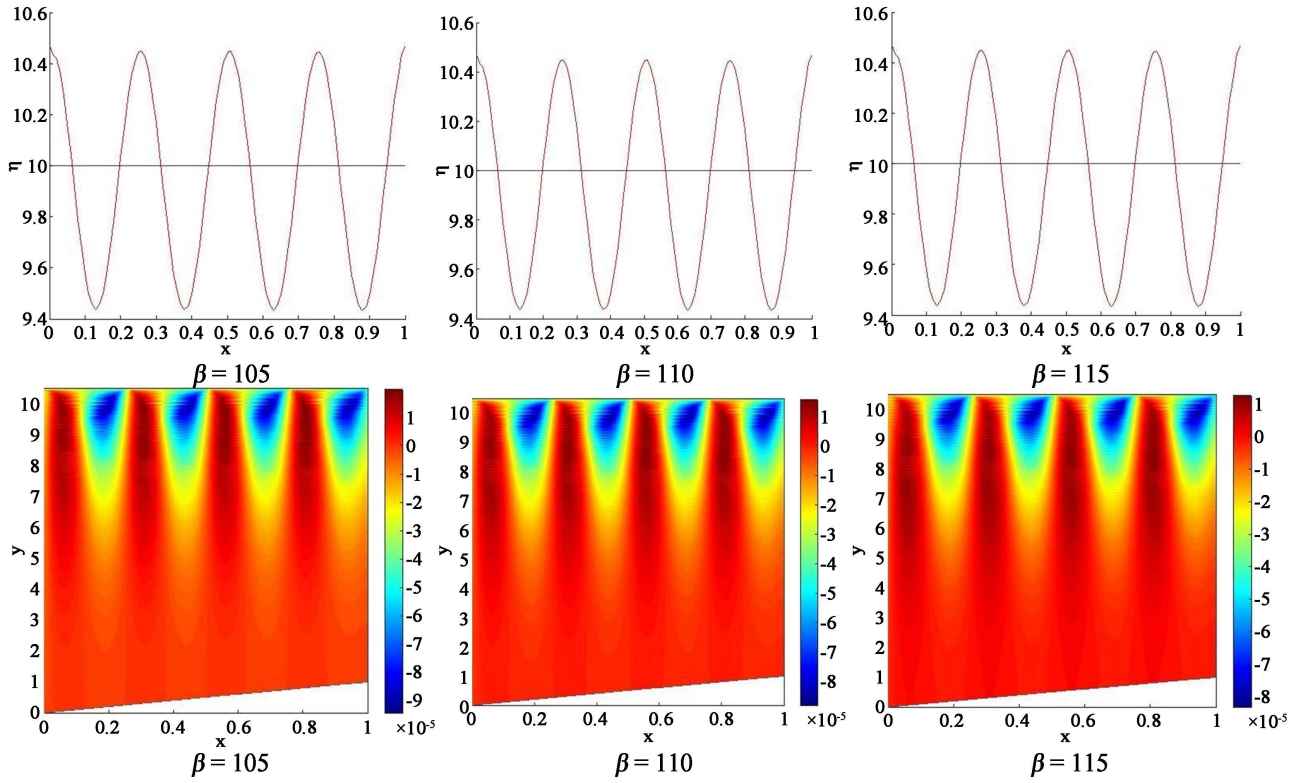

Figure 6. Free surface and velocity potential profiles for $t^* = 0.36$ for different values of β.

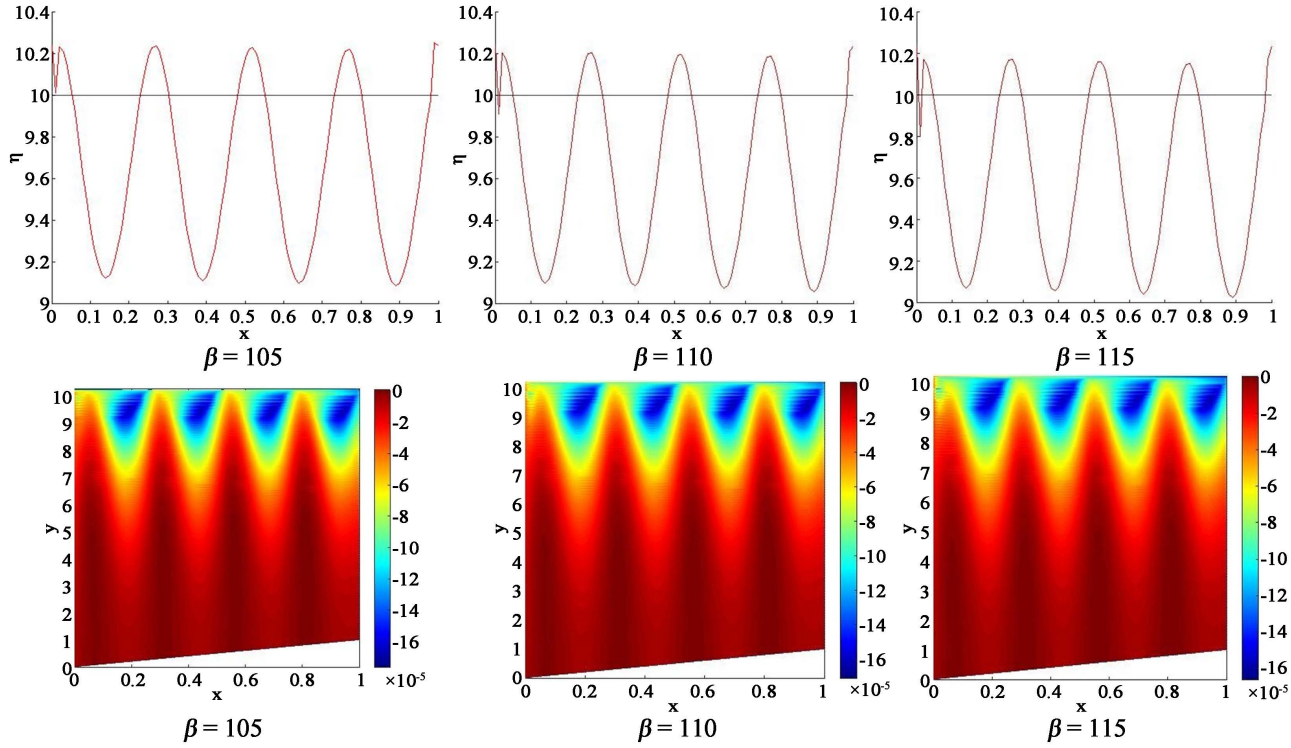

Figure 7. Free surface and velocity potential profiles for $t^* = 1.7$ for different values of β.

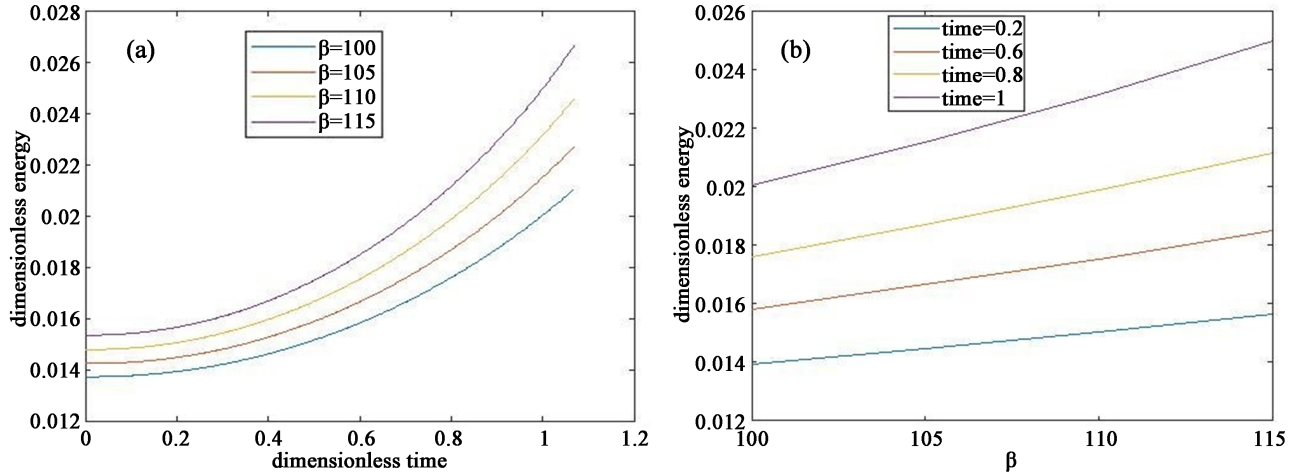

Figure 8. (a) Evolution of the energy over time for each β; (b) Evolution of the energy over β at fixed times.

the movement when β increases. The movement of the particles then stabilizes when the linear slope of the bottom becomes lower and lower.

5.4. Influence of β on Wave Energy

Figure 8 shows respectively the evolution of the energy over time for each β and the influence of the slope on the energy at fixed times.

Figure 8(a) shows that there is an increasing in energy over time for each value of β. The "impermeable wall" exit condition has the effect of reflecting the wave without energy absorption. Thus, the superposition of incident and reflected

waves increases the energy over time.

Figure 8(b) shows that the energy of the wave increases linearly with β. The lower the slope, the higher the energy. This shows that the linear slope of the bottom plays a role in the variation of the energy.

6. Conclusions

A numerical wave tank was studied in this work to observe the effect of a linearly bottom slope on the wave energy contained in a wavelength. For this purpose, we observed a simulation using the nonlinear Stokes theory to describe the calculation in a hydrodynamic approach first. The hydrodynamic results are obtained using the finite difference method.

The numerical simulations show that the particles' movement is influenced by the passage of the Stokes wave. The "impermeable wall" exit condition influences the longitudinal variation of the wave and consequently the particles' movement. Also, the linear slope of the bottom influences the movement of the particles especially at the free surface and the longitudinal profile of the wave in high time by playing an attenuating role when it decreases.

Finally, we deduced from the hydrodynamic results the energetic results by the Newtonian numerical method. We found an increase in energy with time under the assumption of the "impermeable wall" exit condition.

However, we found that with the increase of β, *i.e.* the decrease of the bottom slope that the energy increases. Thus, we get a better energy output when the linear slope of the bottom is low. In the opposite case, we note a decrease in energy due to a frictional interaction with the linear slope of the bottom.

Finally, the "impermeable wall" exit condition and the linear slope of the bottom are important factors to take into account when monitoring the evolution of the hydrodynamic and energy parameters. Our study allowed us to know the ideal location of wave generators (far or close to the coast) as a function of depth by considering a numerical wave channel with a linearly variable bottom. For onshore wave generators, see the studies of Youness and Lafon [27] and offshore those of Drew, Plumer and Sahinkaya [28].

Conflicts of Interest

The authors declare no conflicts of interest regarding the publication of this paper.

References

[1] Bougis, J. (1993) Les houles periodiques simples. Institut des Sciences de l'Ingenieur de Toulon et du Var, Universite' de Toulon et Du Var.

[2] Nayfey, A. (1973) Perturbation Methods. John Wiley and Sons, New York.

[3] Christensen, E.D. and Deigaard, R. (2001) Large Eddy Simulation of Breaking Waves. *Coastal Engineering*, **42**, 53-86. https://doi.org/10.1016/S0378-3839(00)00049-1

[4] Klepsvik, J. (1995) Nonlinear Wave Loads on Offshore Structure. Master of Science in Ocean Engineering, Massachusetts Institute of Technology (MIT), Cambridge,

26-36.

[5] Molin, B., Jamois, E., Lee, C.H. and Newman, J.N. (2005) Nonlinear Wave Interaction with a Square Cylinder. In: 20*th International Workshop on Water Waves and Floating Bodies*, Longyearbyen, 29 May-1 June 2005.

[6] Rahman, M., Bora, S.N. and Satish, M.G. (1999) A Note on Second-Order Wave Forces on a Circular Cylinder in Finite Water Depth. *Applied Mathematics Letters*, **12**, 63-70.https://doi.org/10.1016/S0893-9659(98)00128-1

[7] Bhatta, D.D. (2005) Nonlinear Free Surface Condition Due to Second Order Diffraction by a Pair of Cylinders. *Journal of Applied Mathematics and Computing*, **18**, 171-182.

[8] Yang, Z., Liu, S., Bingham, H.B. and Li, J. (2013) A Second-Order Theory for Coupling 2D Numerical and Physical Wave Tanks: Derivation, Evaluation and Experimental Validation. *Coastal Engineering*, **71**, 37-51. https://doi.org/10.1016/j.coastaleng.2012.07.003

[9] Le Touzé, D., Bonnefoy, F. and Ferrant, P. (2002) Second-Order Spectral Simulation of Directional Wave Generation and Propagation in a 3D Tank. In: 17*th International Workshop on Water Waves and Floating Bodies*, Cambridge, UK, 14-17 April 2002.

[10] Mangoub, G. (1992) Étude numérique de l'interaction tourbillon paroi par une Méthode particules maillage. Thèse de Doctorat, Université Paris VI, Paris.

[11] Loukili, M., Mordane, S. and Chagdali, M. (2016) Formulation Semi Analytique de la propagation non linéaire de la Houle. In: *XIV èmes Journées Nationales Génie Côtier—Génie Civil*, Toulon, 29 Juin-1 Juillet 2016, 57-64.

[12] Susbielles, G., Bratu, C. and Cavanie, A. (1981) Vagues et ouvrages Pétroliers en mer. Publications de l'institut français du pétrole, Paris, 65-70.

[13] Belibassakis, K.A. and Athanassoulis, G.A. (2002) Extension of Second Order Stokes Theory to Variable Bathymetry. *Journal of Fluid Mechanics*, **464**, 35-80. https://doi.org/10.1017/S0022112002008753

[14] Babarit, A. and Mouslim, H. (2013) Récuperation de l'énergie des vagues. Techniques de l'Ingenieur, Paris.

[15] Michard, B., Cosquer, E. and Dufour, G.G. (2014) Projet EMACOP: Évaluation du potentiel houlomoteur de 22 sites français en Manche et Atlantique. In: *Journées Nationales Génie Côtier—Génie Civil*, Dunkerque, 2-4 Juillet 2014, 751-758.

[16] Cheung, J.T. and Childress III, E.F. (2007) Ocean Wave Energy Harvesting Devices. Rapp. Tech. Teledyne Scientific et Imaging LLC, Oaks, CA.

[17] Erikson, M. (2007) Modelling and Experimental Verification of Direct Drive Wave Energy Conversion: Buoy-Generator Dynamics. OCLC: 938423643. Thèse de Doctorat, Acta Universitatis Upsaliensis, Uppsala, 1-61.

[18] Du, Q.J. and Leung, D.Y.C. (2011) 2D Numerical Simulation of Ocean Waves. In: *World Renewable Energy Congress*, Sweden, 8-13 May 2011, 2183-2189.

[19] Wei, G., Kirby, J.T. and Sinha, A. (1999) Generation of Waves in Boussinesq Models Using a Source Function Method. *Coastal Engineering*, **36**, 271-299. https://doi.org/10.1016/S0378-3839(99)00009-5

[20] Chawla, A. and Kirby, J.T. (2000) A Source Function Method for Generation of Waves on Currents in Boussinesq Models. *Applied Ocean Research*, **22**, 75-83. https://doi.org/10.1016/S0141-1187(00)00005-5

[21] Dong, C.M. and Huang, C.J. (2004) Generation and Propagation of Water Waves in a Two-Dimensional Numerical Viscous Wave Flume. *Journal of Waterway, Port, Coast-*

al and Ocean Engineering, **130**, 143-153.
https://doi.org/10.1061/(ASCE)0733-950X(2004)130:3(143)

[22] Lu, Y.J. (2007) Numerical Simulation of Two-Dimensional Overtopping against Seawalls Armored with Artificial Units in Regular Waves. *Journal of Hydrodynamics*, **19**, 322-329. https://doi.org/10.1016/S1001-6058(07)60065-1

[23] Da Silva, E.G. (2007) Méthodes et Analyse Numériques. Engineering School. Institut Polytechnique, Grenoble.

[24] Beuneu, J. (1999) Algorithmes pour le calcul scientifique. Cours de l'Ecole Universitaire d'Ingénieurs, Lille.

[25] Bejan, A. (2013) Convection Heat Transfer. John Wiley & Sons, New York.

[26] Demailly, J.P. (1996) Analyse numérique et équations différentielles. Presses Universitaires, Grenoble.

[27] Elchahal, G., Younes, R. and Lafon, P. (2008) The Effects of Reflection Coefficient of the Harbour Sidewall on the Performance of Floating Breakwaters. *Ocean Engineering*, **35**, 1102-1112.

[28] Drew, B., Plummer, A.R. and Sahinkaya, M.N. (2009) A Review of Wave Energy Converter Technology. *Proceedings of the Institution of Mechanical Engineers*, *Part A*: *Journal of Power and Energy*, **223**, 887-902.

Nomenclature

Latin Letters

A: wave amplitude, m

$C_{r\bar{F}}$: criterion for stopping the temporal iterative process

$e_{\bar{F}}$: relative error of the temporal iterative process

E_p, E_c: potential and kinetic energy over a wavelength, J·m^{-1}

F_r: Froude number

g: gravity intensity, m

$h(x)$: bottom profile, m

h_0: slope height at the exit of the tank, m

H_e: mean height of the tank, m

J: Jacobian of the transformation, m

k; wave number, m^{-1}

L: lenght of the tank, m

t: time, s

x, z: horizontal and vertical coordinates in physical domain, m

Greek Symbols

η: free surface elevation, m

ϕ: velocity potential, m^2·s^{-1}

ω: wave pulse, rad·s^{-1}

λ: wavelength, m

β; parameter providing information on the slope

χ^*, ζ^*: dimensionless horizontal and vertical curvilinear coordinates

$\varepsilon_{\bar{F}}$: criterion for stopping the itterative process

$\bar{F}$: free surface elevation or velocity potential

Superscripts

$*$: related to dimensionless parameters

n: related to time

k: related to number of iteration